



Cite this: *Lab Chip*, 2022, 22, 3663

Received 12th July 2022,
Accepted 30th August 2022

DOI: 10.1039/d2lc00641c

rsc.li/loc

A similarity scaling approach for organ-on-chip devices†

James J. Feng ^{*,ab} and Sarah Hedtrich ^{cde}

Organ-on-chip devices (OoCs) provide more nuanced insights into (patho)physiological processes of the human body than static tissue models, and are currently the most promising approach to emulating human (patho)physiology *in vitro*. OoC designs vary greatly and questions remain as to how to maximize biomimicry and clinical translatability of the *in vitro* findings. Scaling is critical, yet has largely been *ad hoc*, consisting in matching one or a few variables between the OoC and the target organ. This has limited the predictive value of OoCs. Here, we propose a systematic approach based on the principle of similitude widely used in the physical sciences, and present three case studies from the recent literature to demonstrate how the approach works. A lung-on-a-chip and a liver-on-a-chip both satisfied important similarity criteria, and therefore yielded results that were in good agreement with clinical data. A gut–liver system failed to satisfy a key criterion of kinematic similarity, and yielded unphysiological pharmacokinetic responses *in vitro*. The similarity scaling approach promises to improve markedly the design and operation of organ- and human-on-chip devices.

Introduction

The past decade has seen intensifying efforts to develop complex *in vitro* models that closely replicate functions of human organs.^{1,2} These typically involve multiple cell types assembled in three dimensions to mimic the morphology and

functionality of the target organs, and are popularly known as “organ-on-chip” (OoC) devices or microphysiological systems (MPS).^{3–5} Such OoCs can be assembled into a multi-organ-on-chip system to study inter-organ crosstalk.^{6–8} OoCs emulate organ-level (patho)physiology and are currently the most promising human-based approach in biomedical research. Much of this research has been motivated by the prospect of using OoCs to improve clinical translation and reduce attrition rate in the drug development process, potentially replacing animal testing.^{2,3,5,9–13}

For a miniaturized on-chip culture to mimic a human organ, scaling is a central issue: how to design OoCs so that their performance *in vitro* can be extrapolated to the functions of organs *in vivo*? Existing approaches are mostly *ad hoc*, focusing on specific parameters or functions in a specific OoC. In particular, they do not account systematically for the many interlinked mechanisms and parameters in OoCs. For example, direct scaling¹⁴ and allometric scaling¹⁵ use the OoC-to-human size or mass ratio to determine the size of the organs on the chip. Such scalings do not involve any time scales, and cannot ensure proper scaling of rate parameters (*e.g.*, perfusion and metabolic rates). In a gut–liver system, direct or allometric scaling would produce drug exposure times that are orders of magnitude below *in vivo*.¹⁶ Functional scaling strives for *in vivo* levels of key functions for each organ, *e.g.*, metabolic rate for the liver or filtration rate for the kidney.^{17,18} But the difficulty lies in balancing the often conflicting needs of multiple functions, especially in multiple OoCs setups.^{6,16} From the earlier years of OoC development, scaling has been recognized as an outstanding problem.^{3,17,19,20} But a general framework for scaling remains elusive, and recent reviews have consistently listed scaling as an urgent problem to be tackled.^{1,8,21,22}

We argue that the solution requires a shift in focus from the *ad hoc* needs of specific OoCs to a systematic view that accounts for the multiple factors involved. Here we propose one such framework by adapting the techniques of dimensional analysis and similarity, both classical tools in physics and engineering.

^a Department of Chemical and Biological Engineering, University of British Columbia, Vancouver, BC V6T 1Z4, Canada. E-mail: james.feng@ubc.ca

^b Department of Mathematics, University of British Columbia, Vancouver, BC V6T 1Z2, Canada

^c Department of Infectious Diseases and Respiratory Medicine, Charité – Universitätsmedizin Berlin, Corporate member of Freie Universität Berlin and Humboldt Universität zu Berlin, Germany

^d Center of Biological Design, Berlin Institute of Health at Charité – Universitätsmedizin Berlin, Germany

^e Faculty of Pharmaceutical Sciences, University of British Columbia, Vancouver, BC V6T 1Z3, Canada

† Electronic supplementary information (ESI) available. See DOI: <https://doi.org/10.1039/d2lc00641c>



Similarity scaling

In any physical process, if the *output* P is determined by *input* quantities q_i ($i = 1, \dots, n$), then these inputs must be algebraically linked in such a way as to yield the proper dimension of P . The pi theorem²³ asserts that the relationship among P and q_i can be reduced, without any loss of generality, to one among a smaller number of independent dimensionless Π groups, each formed by products of powers of P and q_i . This relationship then forms the basis for scaling between a *model* and its *prototype*. The procedure is widely used in scale-up in physics and engineering,^{24,25} and the ESI† offers an example in aeronautics.

For an OoC, we first identify the key output P that is to be translated to *in vivo*. Then the Π group Π_1 that represents P must be a function of the other Π groups, Π_2, \dots, Π_m ,

$$\Pi_1 = f(\Pi_2, \Pi_3, \dots, \Pi_m),$$

with the total number $m < n + 1$. If we ensure that the inputs Π_2, \dots, Π_m for the OoC match those *in vivo*, the output Π_1 must be matched as well. Thus, we have achieved *similarity* between the OoC and its target organ, and the *in vitro* measurement of P can be translated to the *in vivo* organ. Notably, this does not require knowledge of the function f , which is almost always unknown in a complex system. The procedure can be extended to multiple output functions for a single OoC, or to multi-organ chips.

Similarity criteria

When scaling mechanical systems, one sometimes classifies the dimensionless groups according to geometric, kinematic and dynamic similarity.^{26,27} Geometric similarity governs the Π groups describing length, area and volume ratios, angles and shapes. Such ratios must be equal between the model and the prototype. Kinematic similarity requires equality of time-scale ratios in addition to length ratios. Thus, it concerns Π groups that involve velocity and other rate quantities. On the basis of these two, dynamic similarity further introduces mass ratios so that dynamic quantities such as pressure, shear stresses and forces, which typically constitute the output Π groups in a mechanical system, are scaled properly.

This scheme can be adapted and expanded for scaling OoCs. The Π groups about OoC size, shape and volume pertain to geometric similarity, those about residence time, perfusion rates and kinetic rates belong to kinematic similarity, and finally those involving forces and stresses fall under dynamic similarity. For OoCs, we need to add *morphological similarity* as a new criterion, which ensures the proper structure and morphology of heterotypic cell assemblies, *e.g.*, to distinguish spheroids from dispersed cells, and predominantly 2D from 3D structures.^{19,28} Finally, metabolic outcomes such as concentration profiles are central to pharmacokinetic/pharmacodynamic (PKPD) studies using OoCs.^{16,29,30} Thus, we propose another new criterion

called *metabolic similarity* that ensures proper scaling of dosage and concentrations.

It is also interesting to note that some of the *ad hoc* scaling schemes proposed in earlier work^{8,16,18,19} may be identified with the similarity criteria above. For example, requirements on chamber size ratio and cell number are for geometric similarity. Requirements on perfusion rates, metabolic rates, organ- or cell-to-liquid ratios and residence time concern kinematic similarity, and requirement on shear stress concerns dynamic similarity. Thus, in carrying out the proposed similarity scaling, one may also satisfy some such *ad hoc* criteria by accident.

Partial similarity

In principle, the pi theorem guarantees similarity. In the laboratory, however, complete similarity may not be attainable because of limitations on the materials available, fabrication techniques and accessible experimental conditions. In such cases, one strategically omits certain Π groups and strives for partial similarity.²³ This is often necessary even for mechanical systems. In the OoC, we may have to determine which input Π 's are more or less important for the phenomena of interest, and carry out scaling based on partial similarity. In multi-organ chips, the greater complexity implies a larger number of Π groups. Although the principle of similarity scaling applies to such systems, partial similarity may become unavoidable.

Case studies

Similarity scaling differs from prior scaling methods in that it accounts for all parameters and their interactions in a systematic way. Although OoCs are vastly more complex than mechanical systems, we show here that the success of similarity scaling in the latter can be reproduced in the former, provided that the OoC experiments are designed and executed properly. For this purpose, we have selected three studies from the literature based on the completeness of the reported parameters, operating conditions, and quantitative outputs for their respective OoCs. The availability of such data make them proper test cases for the similarity scaling approach.

Lung-on-a-chip (LOAC)

Huh *et al.*^{31,32} developed the LOAC as a mimic for an alveolus. It features an air-liquid interface that can be cyclically stretched to replicate the alveolar stretching during breathing. As a disease model for pulmonary edema due to cancer treatment by interleukin-2, the LOAC manifests a gradual loss of barrier function; the increase in permeability agrees well with *ex vivo* data from whole mouse lungs.³²

To examine the success of LOAC from the angle of similarity scaling, we take the permeability to be the output that depends on a host of input variables and parameters, including the drug dosage, the frequency and amplitude of



membrane stretching, and the medium perfusion velocity. Our dimensional analysis (see ESI† for details) produces 6 Π groups, with the output $\Pi_1 = k/D^2$ being the ratio of the membrane permeability to the chamber width squared. The authors have matched the Π groups between the LOAC and *in vivo*. In particular, the following similarity criteria are satisfied:

- Geometric similarity: the LOAC matches the chamber size and the air–liquid–interface thickness with the alveolus *in vivo*.
- Morphological similarity: the LOAC has confluent endothelial and epithelial monolayers apposed on either side of the membrane, approximating the air–blood boundary *in vivo*.
- Kinematic similarity: the membrane stretching amplitude, frequency and the medium perfusion velocity are all chosen to match the *in vivo* conditions.
- Metabolic similarity: the interleukin-2 dosage and application time are matched with *in vivo* conditions.

Thus, the LOAC and the operating conditions of Huh *et al.*³² have achieved similarity with the *in vivo* counterpart. This ensures that the output of the LOAC, the membrane permeability enhanced by interleukin-2 treatment, is translatable from the LOAC to the alveolus. Note that this is a somewhat special case of 1:1 size ratio between the model and the prototype. Moreover, all the Π groups are matched for a rare attainment of complete similarity.

More recently, second-generation LOACs have been developed that continue to maintain similarity scaling with a 1:1 size ratio, but with improved and refined features, including the use of primary alveolar epithelial cells instead of a cell line³³ and the modeling of cytokine production and leukocyte recruitment following an influenza infection.³⁴

Liver-on-a-chip

Ewart *et al.*³⁵ studied drug-induced liver injury (DILI) on a Liver-Chip, an OoC that models a liver sinusoid. Judging by suppressed albumin production and other symptoms, the OoC distinguished toxic drugs from their non-toxic structural analogs, and correctly ordered the toxicity of drugs according to the Garside DILI rank. We will demonstrate below that this success is again rooted in satisfying similarity scaling to the *in vivo* organ, which is the human liver sinusoid in this case.

The details of the dimensional analysis can be found in the ESI† and only a brief summary is given below. Without drug treatment, the Liver-Chip produces albumin *in vitro* in the physiologic *in vivo* range of 20–105 μg per 10^6 hepatocytes per day. In the DILI study, therefore, the main output is the albumin production as a fraction of the control without drug treatment: $\Pi_1 = \phi$. The input variables and parameters are listed in Table 1, along with the values of the input Π groups, Π_2, \dots, Π_5 . Of these, Π_2, Π_3 and Π_4 match reasonably well between *in vitro* and *in vivo*. Π_5 differs considerably, but its small magnitudes suggest that permeation through the cell layers happens rapidly, and is not the rate-limiting step. Thus, we can disregard Π_5 and claim partial similarity

Table 1 Similarity scaling for the Liver-Chip in a DILI study.³⁵ The input parameters are L : chip dimension, u : perfusion velocity, c : initial drug concentration, c_{50} : required drug concentration to produce a 50% reduction in albumin, D : drug diffusivity in perfusate, P : permeability through the membrane, k : drug clearance rate. The various rates are for the drug diclofenac. See ESI† for details of dimensional analysis and the sources for the parameter values

| Parameters | <i>In vitro</i> values | <i>In vivo</i> values |
|---|------------------------|-----------------------|
| L (μm) | 200 | 5 |
| u ($\mu\text{m min}^{-1}$) | 2500 | 6.67×10^4 |
| k ($\mu\text{m}^3 \text{min}^{-1}$) | 1.67×10^9 | 2.93×10^7 |
| D ($\mu\text{m}^2 \text{min}^{-1}$) | 4.50×10^4 | 4.50×10^4 |
| P ($\mu\text{m min}^{-1}$) | 6.53×10^6 | 6.53×10^6 |
| c (μM) | 0.05 | 0.05 |
| c_{50} (μM) | 0.1 | 0.1 |
| $\Pi_2 = c/c_{50}$ | 0.5 | 0.5 |
| $\Pi_3 = uL^2/k$ | 5.99×10^{-2} | 5.69×10^{-2} |
| $\Pi_4 = uL/D$ | 11.1 | 7.41 |
| $\Pi_5 = u/P$ | 3.83×10^{-4} | 1.02×10^{-2} |

between the Liver-Chip and the liver sinusoid *in vivo*. This ensures translatability of albumin suppression $\Pi_1 = \phi$, and therefore the proper detection of DILI.

Even though the Liver-Chip is much larger than the liver sinusoid *in vivo*, the perfusion and drug clearance rates also differ so as to compensate through the Π groups. This systematic treatment is the principal advantage of similarity scaling over prior scaling that focuses on matching individual parameters.

Gut–liver system

Cirit *et al.*^{16,36,37} linked a gut and a liver module into a multi-OoC system that captured the key functions of both organs—the permeation of orally administered drugs across the membrane in the gut and drug metabolism in the liver—as well as their crosstalk. The gut OoC has an apical chamber and a basolateral chamber, but the liver OoC has a single chamber. Both are connected to a mixing chamber that supplies the common perfusion. This system has been used to study drug metabolism in a multi-organ system.^{16,37}

The system involves a larger number of parameters, and requires a lengthier dimensional analysis resulting in 12 Π groups (details in ESI†). For the present purpose, we need only discuss the parameters and Π groups relevant to kinematic similarity, more specifically the transport and kinetic rates. These are listed in Table 2 for the drug diclofenac. The dimensionless groups Π_6 and Π_7 indicate the gut and liver metabolic rates of the drug relative to its transport rate by perfusion. Π_8 gives the ratio between the drug permeation and perfusion. The small values of C_g and Π_6 indicate negligible drug metabolism in the gut. The most prominent discrepancy is in $\Pi_7 = C_l/Q$, which is more than 10 000 times greater *in vitro* than *in vivo*. This severely violates the kinematic similarity.²³ Π_7 is also the ratio between the circulation time $T_0 = V_m/Q$ and the liver clearance time $T_1 = V_m/C_l$. Not only is the circulation too slow



Table 2 Similarity scaling for a gut–liver OoC system,^{16,37} with a partial list of the rate parameters: C_l and C_g : diclofenac clearance rates in liver and gut, P : membrane permeability, Q : perfusion rate, S : membrane area, V_m : volume of mixing chamber, T_0 : circulation time, T_l : liver clearance time. See ESI† for details of dimensional analysis and the sources for the parameter values

| Parameters | <i>In vitro</i> values | <i>In vivo</i> values |
|-------------------------------|------------------------|-----------------------|
| C_l (mL min ⁻¹) | 0.0102 | 0.0813 |
| C_g (mL min ⁻¹) | 0.00029 | 0 |
| P (cm min ⁻¹) | 8.83×10^{-4} | 1.08×10^{-3} |
| Q (mL min ⁻¹) | 0.0104 | 1250 |
| S (cm ²) | 1.12 | 3×10^5 |
| V_m (mL) | 1 | 1750 |
| $\Pi_6 = C_g/Q$ | 0.0279 | 0 |
| $\Pi_7 = C_l/Q$ | 0.980 | 6.50×10^{-5} |
| $\Pi_8 = PS/Q$ | 0.0951 | 0.259 |
| $T_0 = V_m/Q$ (min) | 96.1 | 1.40 |
| $T_l = V_m/C_l$ (min) | 98.0 | 21 525 |

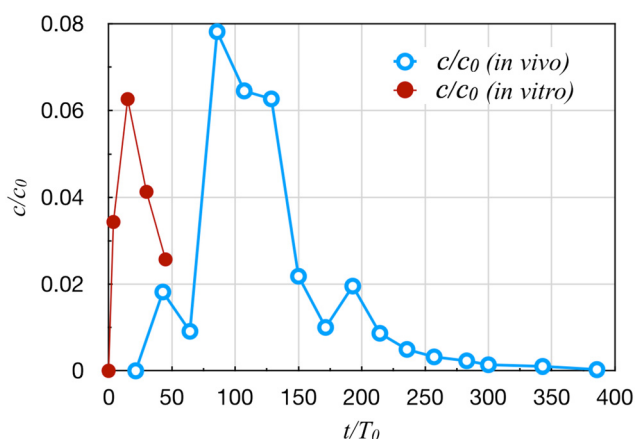


Fig. 1 Comparison of the plasma diclofenac concentration profiles *in vivo*¹⁶ and *in vitro*.³⁷ Time t is scaled by the circulation time T_0 , and concentration c by the initial concentration c_0 in the dosing chamber.

in vitro, the clearance is also too fast. As a result, the time concentration profile fails to translate to the clinical data, with a much shorter time scale than *in vivo* (Fig. 1).¹⁶

Similarity scaling not only pinpoints the cause of the mis-scaling, but can also suggest ways to correct it. Since C_l depends on the metabolism of individual cells, it cannot be easily varied *in vitro*. Thus one can only raise the perfusion rate Q to lower Π_7 . To maintain the value of Π_8 , already roughly matched with *in vivo*, one must increase the gut epithelial area S in proportion to Q . This systematic approach to managing the parameters is the hallmark of similarity scaling.

Discussion

Similarity scaling offers a systematic scheme for matching OoCs and their target organs, as opposed to matching individual parameters. It is also mathematically guaranteed to work by the pi theorem. In practice, limitations in available materials and fabrication techniques often make complete

similarity impossible. But even partial similarity can provide highly useful guidelines, as demonstrated in the above.

OoCs being biological systems puts special constraints on similarity scaling. An individual cell is in a sense the minimum unit and cannot be scaled further down. Thus, an OoC typically contains a smaller number of the same cells as *in vivo*, not the same number of “smaller cells” as perfect similarity would dictate. Moreover, certain parameters, *e.g.*, cellular metabolic rates, will be more or less fixed at their *in vivo* values and not subject to large variations for scaling. Despite these limitations, we have shown the utility and potential of similarity scaling in the case studies. It will offer a general framework for designing the next generation of organ- and human-on-chip systems.

Materials and methods

The method of dimensional analysis is illustrated with examples in the ESI†, which also contains detailed analysis and all the data for the three case studies.

Author contributions

JJF and SH conceptualized the project, carried out the investigation, analyzed the data and wrote the paper.

Conflicts of interest

There are no conflicts to declare.

Acknowledgements

We acknowledge partial funding of this work from the Stiftung Charité (S. H.), the Natural Sciences and Engineering Research Council Canada (2020-04224 for S. H., 2019-04162 for J. J. F.), the German Research Foundation (DFG, SFB 1449-431232613, project A5, S. H.), and the John R. Evans Leaders Fund (S. H.). J. J. F. thanks Milica Radisic (University of Toronto) for suggesting the scaling problem to him. The image in the online “Table of Contents” entry was partly generated using Servier Medical Art, provided by Servier, licensed under a Creative Commons Attribution 3.0 unported license.

Notes and references

- G. Vunjak-Novakovic, K. Ronaldson-Bouchard and M. Radisic, *Cell*, 2021, **184**, 4597–4611.
- L. A. Low, C. Mummery, B. R. Berridge, C. P. Austin and D. A. Tagle, *Nat. Rev. Drug Discovery*, 2021, **20**, 345–361.
- K. Ronaldson-Bouchard and G. Vunjak-Novakovic, *Cell Stem Cell*, 2018, **22**, 310–324.
- S. E. Park, A. Georgescu and D. Huh, *Science*, 2019, **364**, 960–965.
- M. Weinhart, A. Hocke, S. Hippenstiel, J. Kurreck and S. Hedtrich, *Pharmacol. Res.*, 2019, **139**, 446–451.
- J. H. Sung, Y. I. Wang, S. N. Narasimhan, M. Jackson, C. Long, J. J. Hickman and M. L. Shuler, *Anal. Chem.*, 2019, **91**, 330–351.



- 7 D. Park, J. Lee, J. J. Chung, Y. Jung and S. H. Kim, *Trends Biotechnol.*, 2020, **38**, 99–112.
- 8 M. Malik, Y. Yang, P. Fathi, G. J. Mahler and M. B. Esch, *Front. Cell Dev. Biol.*, 2021, **9**, 721338.
- 9 N. T. Elliott and F. Yuan, *J. Pharm. Sci.*, 2011, **100**, 59–74.
- 10 U. Marx, T. Akabane, T. B. Andersson, E. Baker, M. Beilmann, S. Beken, S. Brendler-Schwaab, M. Cirit, R. David, E. M. Dehne, I. Durieux, L. Ewart, S. C. Fitzpatrick, O. Frey, F. Fuchs, L. G. Griffith, G. A. Hamilton, T. Hartung, J. Hoeng, H. Hogberg, D. J. Hughes, D. E. Ingber, A. Iskandar, T. Kanamori, H. Kojima, J. Kuehn, M. Leist, B. Li, P. Loskill, D. L. Mendrick, T. Neumann, G. Pallocca, I. Rusyn, L. Smirnova, T. Steger-Hartmann, D. A. Tagle, A. Tonevitsky, S. Tsyb, M. Trapecar, B. Van de Water, J. Van den Eijnden-van Raaij, P. Vulto, K. Watanabe, A. Wolf, X. Zhou and A. Roth, *ALTEX*, 2020, **37**, 365–394.
- 11 P. P. Adhikary, Q. U. Ain, A. C. Hocke and S. Hedtrich, *Nat. Rev. Mater.*, 2021, **6**, 374–376.
- 12 B. Cecen, C. Karavasili, M. Nazir, A. Bhusal, E. Dogan, F. Shahriyari, S. Tamburaci, M. Buyukoz, L. D. Kozaci and A. K. Miri, *Pharmaceutics*, 2021, **13**, 1657.
- 13 K. Ronaldson-Bouchard, D. Teles, K. Yeager, D. N. Tavakol, Y. Zhao, A. Chramiec, S. Tagore, M. Summers, S. Stylianou, M. Tamargo, B. M. Lee, S. P. Halligan, E. H. Abaci, Z. Guo, J. Jacków, A. Pappalardo, J. Shih, R. K. Soni, S. Sonar, C. German, A. M. Christiano, A. Califano, K. K. Hirschi, C. S. Chen, A. Przekwas and G. Vunjak-Novakovic, *Nat. Biomed. Eng.*, 2022, **6**, 351–371.
- 14 I. Maschmeyer, A. K. Lorenz, K. Schimek, T. Hasenberg, A. P. Ramme, J. Hübner, M. Lindner, C. Drewell, S. Bauer, A. Thomas, N. S. Sambo, F. Sonntag, R. Lauster and U. Marx, *Lab Chip*, 2015, **15**, 2688–2699.
- 15 A. Ahluwalia, *Sci. Rep.*, 2017, **7**, 42113.
- 16 C. Maass, C. L. Stokes, L. G. Griffith and M. Cirit, *Integr. Biol.*, 2017, **9**, 290–302.
- 17 J. P. Wikswo, E. L. Curtis, Z. E. Eagleton, B. C. Evans, A. Kole, L. H. Hofmeister and W. J. Matloff, *Lab Chip*, 2013, **13**, 3496–3511.
- 18 J. H. Sung, Y. Wang and M. L. Shuler, *APL Bioeng.*, 2019, **3**, 021501.
- 19 C. Moraes, J. M. Labuz, B. M. Leung, M. Inoue, T.-H. Chun and S. Takayama, *Integr. Biol.*, 2013, **5**, 1149–1161.
- 20 C. L. Stokes, M. Cirit and D. A. Lauffenburger, *CPT: Pharmacometrics Syst. Pharmacol.*, 2015, **4**, 559–562.
- 21 P. Sphabmixay, M. S. B. Raredon, A. J.-S. Wang, H. Lee, P. T. Hammond, N. X. Fang and L. G. Griffith, *Biofabrication*, 2021, **13**, 045024.
- 22 D. E. Ingber, *Nat. Rev. Genet.*, 2022, **23**, 467–491.
- 23 M. Zlokarnik, *Scale-Up in Chemical Engineering*, WILEY-VCH Verlag, 2nd edn, 2006.
- 24 A. Bisio and R. L. Kabel, *Scale-up of Chemical Processes: Conversion from Laboratory Scale Tests to Successful Commercial Size Design*, Wiley-Interscience, 1985.
- 25 J. M. Bonem, *Chemical Projects Scale Up: How to Go from Laboratory to Commercial*, Elsevier, 2018.
- 26 J. R. Welty, C. E. Wicks, R. E. Wilson and G. L. Rorrer, *Fundamentals of Momentum, Heat, and Mass Transfer*, Wiley, 5th edn, 2008, pp. 125–136.
- 27 F. M. White, *Fluid Mechanics*, McGraw-Hill, Seventh edn, 2011, pp. 293–345.
- 28 N. Ucciferri, T. Sbrana and A. Ahluwalia, *Front. Bioeng. Biotechnol.*, 2014, **2**, 74.
- 29 C. Ma, Y. Peng, H. Li and W. Chen, *Trends Pharmacol. Sci.*, 2021, **42**, 119–133.
- 30 Y. Yang, Y. Chen, L. Wang, S. Xu, G. Fang, X. Guo, Z. Chen and Z. Gu, *Front. Bioeng. Biotechnol.*, 2022, **10**, 900481.
- 31 D. Huh, B. D. Matthews, A. Mammoto, M. Montoya-Zavala, H. Y. Hsin and D. E. Ingber, *Science*, 2010, **328**, 1662–1668.
- 32 D. Huh, D. C. Leslie, B. D. Matthews, J. P. Fraser, S. Jurek, G. A. Hamilton, K. S. Thorne, M. A. McAlexander and D. E. Ingber, *Sci. Transl. Med.*, 2012, **4**, 159ra147.
- 33 P. Zamprogno, S. Wüthrich, S. Achenbach, G. Thoma, J. D. Stucki, N. Hobi, N. Schneider-Daum, C.-M. Lehr, H. Huwer, T. Geiser, R. A. Schmid and O. T. Guenat, *Commun. Biol.*, 2021, **4**, 168–423.
- 34 H. Bai, L. Si, A. Jiang, C. Belgur, R. Plebani, C. Oh, M. Rodas, A. Nurani, S. Gilpin, R. K. Powers, G. Goyal, R. P. Baun and D. E. Ingber, *Nat. Commun.*, 2022, **13**, 1928.
- 35 L. Ewart, A. Apostolou, S. A. Briggs, C. V. Carman, J. T. Chaff, A. R. Heng, S. Jadalannagari, J. Janardhanan, K.-J. Jang, S. R. Joshipura, M. Kadam, M. Kanellias, V. J. Kujala, G. Kulkarni, C. Y. Le, C. Lucchesi, D. V. Manatakis, K. K. Maniar, M. E. Quinn, J. S. Ravan, A. C. Rizo, J. F. Sauld, J. Sliz, W. Tien-Street, D. Ramos Trinidad, J. Velez, M. Wendell, P. K. Mahalingaiah, D. E. Ingber and D. Levner, *bioRxiv*, 2021, preprint, DOI: [10.1101/2021.12.14.472674](https://doi.org/10.1101/2021.12.14.472674).
- 36 N. Tsamandouras, T. Kostrzewski, C. L. Stokes, L. G. Griffith, D. J. Hughes and M. Cirit, *J. Pharmacol. Exp. Ther.*, 2017, **360**, 95–105.
- 37 N. Tsamandouras, W. L. K. Chen, C. D. Edington, C. L. Stokes, L. G. Griffith and M. Cirit, *AAPS J.*, 2017, **19**, 1499–1512.

